Rate constants for the CO_2 02^00-10^00 relaxation*

Ralph R. Jacobs, Kenneth J. Pettipiece, and Scott J. Thomas
Lawrence Livermore Laboratory, University of California, Livermore, California 94550
(Received 15 July 1974)

An absorption-cell technique is utilized to determine the rate constants for the CO_2 02^00-10^00 relaxation in CO_2 and binary-gas mixtures of CO_2-He and CO_2-N_2. The experiment consists of injecting a ~2-nsec 10.4-μm pulse through the absorption cell—saturating the CO_2 10^00 to 00^01 transition, and monitoring the subsequent molecular re-equilibrations by recording the temporal intensity of a spatially overlapping probe beam in the 9.4-μm band connecting the 02^00 and 00^01 states. The measured rate constants are $k_{CO_2\text{-}CO_2} = 3 \pm 1$, $k_{CO_2\text{-He}} = 0.8 \pm 0.3$, and $k_{CO_2\text{-}N_2} = 3 \pm 1$, all in units of 10^5 sec^{-1} Torr^{-1}. The experimental approach also yields information on the thermalization of other processes having slower rates, and these are discussed qualitatively. Finally, a comparison is made with other related experimental investigations and two calculations which predict values for $k_{CO_2\text{-}CO_2}$ appreciably different from those measured.

I. INTRODUCTION

The recent strong interest in properties of the CO_2 molecule is in large part motivated by its usefulness as a gain medium in various laser applications. Because of this motivation, the CO_2 molecule has in turn provided a fertile area in which theories on the physics of collisions, energy transfer, and light interaction with inverted and noninverted level populations have been tested.[1]

To add to this wealth of information, we report on the first direct determination of the rate constant k describing the re-equilibration of the CO_2 02^00 and 10^00 vibrational levels. As will be discussed later, the measured rate constant in pure CO_2, $k_{CO_2\text{-}CO_2}$, lies between the predictions of one theory based on short-range interaction forces and another theory based on long-range interactions. The present results thus indicate a need to reformulate certain aspects of these alternate descriptions of the collisional processes in CO_2. From a practical point of view, these rate-constant values determine the deactivation of the lower level in CO_2 molecular amplifiers and thus provide additional information in assessing the performance of such gain media.

II. EXPERIMENTAL APPROACH

In Fig. 1 is shown a partial energy-level diagram for the states of interest in the CO_2 molecule. The levels denoted by 10^00 (symmetric stretch mode) and by 02^00 (bending mode) have eigenfunctions that are strongly mixed because of anharmonic terms in the potential energy, i.e., Fermi resonance.[2] The wave functions for these mixed states can be expressed as linear combinations of the simple harmonic oscillator eigenfunctions 10^00 and 02^00 with roughly equal admixtures of the "pure" state wave functions. However, for brevity throughout the text, these mixed-state wave functions, customarily designated as $[(10^00)\text{-}(02^00)]_I$ at 1388.3 cm^{-1} and $[(10^00)\text{-}(02^00)]_{II}$ at 1285.5 cm^{-1}, will be labeled as 10^00 and 02^00, respectively.

The experiment consists of perturbing the Boltzmann distribution of levels 10^00 and 00^01 in a CO_2 absorption cell, by injection of a short and intense laser pulse in the 10.4-μm band while a second, much longer, probe laser beam in the 9.4-μm band monitors the population difference between the 02^00 and 00^01 states. In particular, the 9.4-μm probe beam gives the temporal population excursions of the 02^00 level since the collisional deactivation rate of the 00^01 state is relatively much longer. The primary re-equilibration process one observes is

$$CO_2(02^00) + M \rightarrow CO_2(10^00) + M - 102.8 \text{ cm}^{-1}, \quad (1)$$

where M can be CO_2, He, or N_2.

A diagrammatical description of the experimental approach is given in Fig. 2. In the experiment a ~2-nsec 10.4-μm saturating pulse containing about six rotational-vibrational transitions, i.e., $P(12)$-$P(22)$, is directed into a 2-m-long×1-in.-diam absorption cell heated to 100°C. Details of the oscillator and single-pulse switchout are given in Ref. 3. The cell is capped at each end by an antireflection-coated NaCl window (reflection <1% at 10.4 μm) and held in place by a low-vapor-pressure epoxy. The temperature across the length of the tube varied by less than 1°C except for the two ends, where the temperature was lower over a distance of about 1 cm. Care was taken prior to experimentation by extensive baking and pumping of the tube and use of pure gases to ensure that any contaminant gas concentration was minimized. Total impurity con-

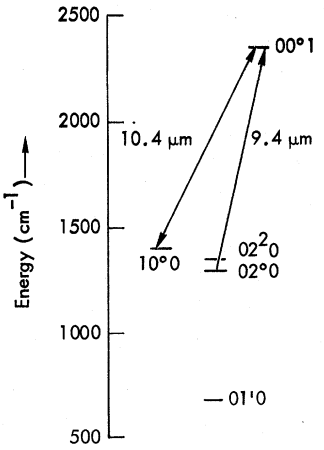

FIG. 1. Energy-level diagram for the relevant, low-lying vibrational states in CO_2.

centration was less than one part per thousand. The probe beam was set at the $P(24)$ transition in the 9.4-μm band. The orthogonally polarized saturating and probe beams were combined at an angled, 0.5-in.-thick germanium plate so that they both were spatially overlapping as they passed through the absorption cell. A suitably positioned diffraction grating and a pair of Brewster angle plates were placed at the exit of the absorption cell to help separate the signals at the two laser frequencies. Finally, the probe beam entered a screen room, passed through a grating monochromator and was detected by a Ge:Hg detector whose output was amplified by a C-Cor preamplifier (3 nsec risetime) and displayed on a Tektronix 7904 oscilloscope (7A13 plug-in). In practice, the probe beam was chopped by a rotating wheel into a 1-msec-long pulse and the 2-nsec, 10.4-μm pulse was introduced during this interval by a previously described triggering technique.[4] The pulse generated by the mode-locked TEA (transversely excited, atmospheric pressure) oscillator was amplified by two TEA amplifiers (Lumonics 103) to about 0.1 J. In the early stages of the experiment, a much weaker 9.4-μm component was detected in the oscillator pulse. To remove any complications in the data interpretations, a 20-cm-long cell filled with CF_2=CFCl at a pressure of 24 Torr[5] was used to remove the 9.4-μm constituent with negligible effect on the 10.4-μm component.

III. DATA AND RESULTS

In Fig. 3 is shown a typical oscilloscope trace depicting the temporal behavior of the transmitted $P(24)$ 9.4-μm probe-beam intensity. For the time scale used in the photograph, at least three distinct signal components can be seen. In Fig. 4, an oscilloscope trace is given on a more expanded time scale to indicate the initial signal increase depicted in Fig. 3. The increasing transmitted signal intensity of Fig. 4 is identified as the collisional process given by Eq. (1) since the trace denotes a *decreasing* 02^00 population, i.e., decreasing absorption. This identification is made on the basis that only this process can occur initially after absorption of the 10.4-μm pulse since the collisional deactivation rate of the upper 00^01 level is well known[6] and has a rate constant of $\sim 3.7\times10^2$ sec^{-1} Torr^{-1}—much longer than that exhibited by the signal of Fig. 4. In fact, a fit was made to data like that shown in Fig. 3 for the slowest decay at long times, and good agreement was obtained for the rate constant k_{00^01} measured

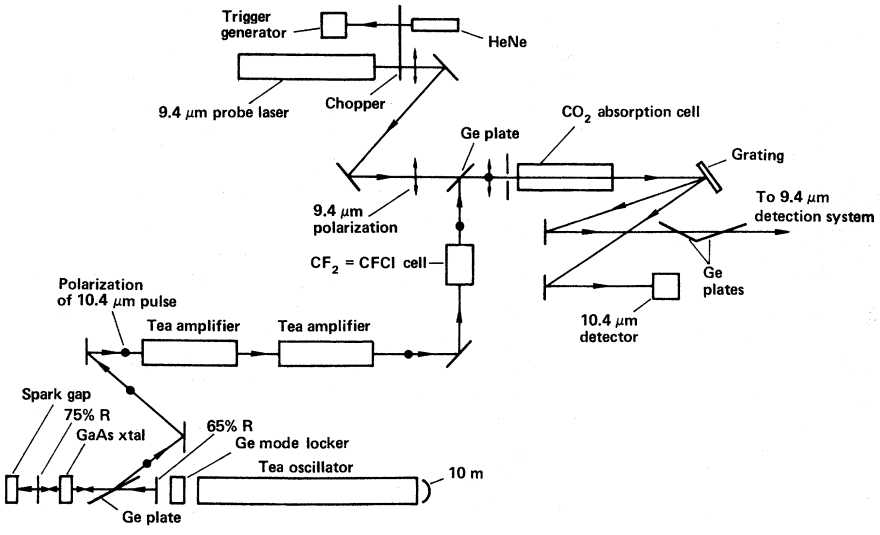

FIG. 2. Schematic diagram of the experimental arrangement (not to scale).

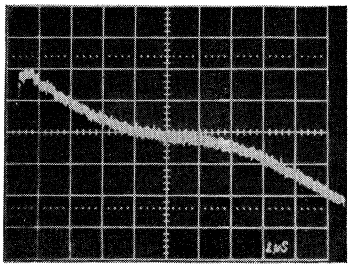

FIG. 3. Shown is an oscilloscope trace for the transmitted $P(24)$ 9.4-μm probe-beam intensity subsequent to absorption of the 10.4-μm pulse for a CO_2 pressure of 100 Torr. The rapid initial rise corresponds to the mechanism given by Eq. (1). The other signal features are discussed in the text.

in Ref. 6. Of course, rotational relaxation phenomena within the 00^01 rotational manifold could contribute to the waveform of Fig. 4; however, they proceed at a rate much faster than that indicated in Fig. 4, and a steady state for this process is attained very rapidly.[3,7] The signal components between the fastest and slowest ones in Fig. 3 are due to processes repopulating the 02^00 level such as

$$01^10 + 01^10 \rightarrow 02^00 + 00^00 + 50.1\ \text{cm}^{-1}, \quad (2)$$

and

$$02^20 + M \rightarrow 02^00 + M + 49.9\ \text{cm}^{-1}, \quad (3)$$

and are considered further in Sec. IV.

Data similar to Fig. 4, corresponding to the mechanism of Eq. (1), were taken for three absorption-cell cases: (i) varied CO_2 pressure, (ii) CO_2 pressure fixed at 50 Torr and He pressure varied, and (iii) CO_2 pressure fixed at 50 Torr and varied N_2 pressure. The data exemplified by Fig. 4 were digitized by a manual scanner and computer fitted by a single exponential function

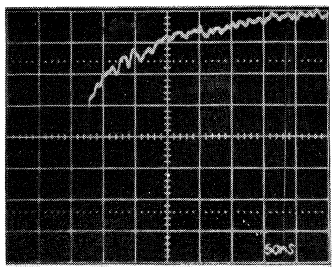

FIG. 4. Depicted is a typical oscilloscope trace for the 02^00-10^00 relaxation in CO_2 (50 Torr). This signal is an expansion of the initial signal rise in Fig. 3. Note that the probe laser baseline is offset from view in Figs. 3 and 4.

to about one e-folding time. The signals for longer times were not included in the fitting to avoid the complications from the subsequent 02^00 repopulating processes.

Since various mechanisms are involved in altering the post-perturbation temporal population of the 02^00 level, the final justification for a one-exponential description of the signal rise shown in Fig. 4 lies in the quality of the fit. The least-squares-fitting function utilizing the single-exponential time-constant parameter gave good agreement with the data with the statistical uncertainty in this parameter, typically a few percent or less. The reduced data for the three cases are shown in Fig. 5, in which the inverse of the fitted relaxation time $1/\tau$ is plotted as a function of pressure. The slopes of the straight lines obtained from a least-squares computer program give the rate constants for the 02^00-10^00 relaxation: $k_{CO_2\text{-}CO_2} = 3 \pm 1$, $k_{CO_2\text{-He}} = 0.8 \pm 0.3$, and $k_{CO_2\text{-}N_2} = 3 \pm 1$ all in units of 10^5 sec^{-1} Torr^{-1}. Self consistency of the mixed-gas results is seen by the agreement of the intercepts with the values predicted by $k_{CO_2\text{-}CO_2} P_{CO_2}$, where $P_{CO_2} = 50$ Torr. The stated error bars ($\pm 1\ \sigma$) account both for statistical fluctuations in the data and a small systematic effect seen among various data runs determining the rate constants. The intermediate rates evident in Fig. 3 were not quantitatively evaluated due to poor signal-to-noise ratios. However, one reasonably concludes that these rate constant values lie between 3×10^5 sec^{-1} Torr^{-1} and 4×10^2 sec^{-1} Torr^{-1} for the pure CO_2 case—the rates for the two limiting processes in Fig. 3.

IV. DISCUSSION

A. Comparison with other experiments

Much work has been reported on the collisional deactivation of the various CO_2 energy levels depicted in Fig. 1 with CO_2 and other gaseous species.[1] Until now, the deactivation process represented by Eq. (1) has not been directly measured. However, we discuss three reported efforts whose results relate to the re-equilibration mechanism illustrated by Eq. (1).

Recently, Stark[8] cited a rate constant for the reverse reaction of Eq. (1) by monitoring the gain in the 9.4-μm and 10.4-μm bands in a CO_2 amplifier after passage of a saturating pulse in the 10.4-μm band. Different temporal gain behaviors for the 9.4- and 10.4-μm bands were observed and the difference was ascribed to the effect of the 10^00-02^00 collisional coupling rate. A rate-equation model describing the population inversion was used to *infer* the rate-constant value from the gain data.

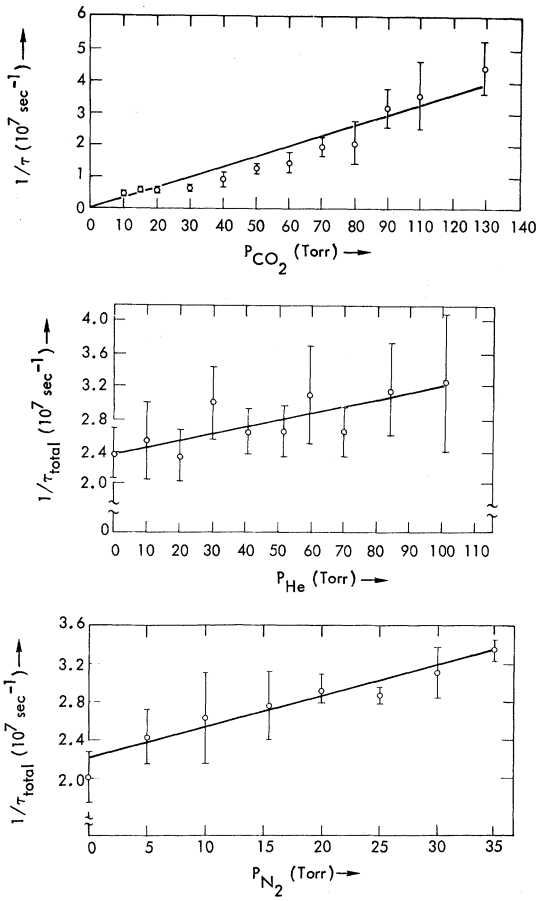

FIG. 5. Linear least-squares fit to the inverse of the fitted relaxation time, $1/\tau$, vs pressure for the three cases: (i) CO_2 alone, (ii) CO_2 fixed at 50 Torr and varied He pressure, and (iii) CO_2 fixed at 50 Torr and varied N_2 pressure. The error flags express ±1 standard deviation for repeated measurements taken under fixed experimental conditions.

Even though the measurement was performed at a single amplifier pressure consisting of a tripartite mixture of CO_2, He, and N_2, a pressure dependence was obtained by scaling the relative contributions of the three gases to the relaxation process according to the ratios of their collisional frequencies with CO_2 and their masses. The reported rate value is:

$$K(10^00\text{-}02^00) = (1.42 \pm 0.5)\times 10^5[P_{CO_2} + 0.46P_{N_2} + 0.054P_{He}]\ \text{sec}^{-1},$$

where the pressures P are in Torr at 400°K. As Sharma[9] indicates, the rate for the reverse reaction should be lower by a factor of 1.45. Thus, Stark's rate-constant value for the process of Eq. (1), in pure CO_2, should be 0.98×10^5 sec^{-1} Torr^{-1}, whereas by contrast our directly determined value is three times larger. Greater discrepancies exist for $k_{CO_2\text{-}He}$ and $k_{CO_2\text{-}N_2}$.

Rhodes, Kelly, and Javan[10] measured a rate constant in pure CO_2 of $(4 \pm 1)\times 10^5$ sec^{-1} Torr^{-1} for the stated processes

$$10^00 \text{ (or } 02^00) + 00^00 \rightleftharpoons 01^10 + 01^10, \tag{4}$$

or

$$10^00 + 00^00 \rightleftharpoons 02^20 + 00^00. \tag{5}$$

Their experiment was similar to the present one in that the 02^00-00^01 transition was saturated in a pure-CO_2 cell with a Q-switched laser pulse in the 9.4-μm band. An absorbed probe laser beam operating in the 10.4-μm CO_2 band monitored the temporal variations of the difference in population densities for the 00^01 and 10^00 states. The time resolution of the experiment was 1 μsec compared to 3 nsec in the present case. Stark[8] suggests that the operative mechanism in this work could be redesignated as the reverse of Eq. (1) instead of either Eqs. (4) or (5). In that case, good agreement exists with the present evaluation for $k_{CO_2\text{-}CO_2}$. In fact, for the reverse reaction of Eq. (1), and correcting for our higher operating temperature, we predict a rate constant for the 10^00-02^00 equilibration of 4×10^5 sec^{-1} Torr^{-1} at their operating temperature.

DeTemple, Suhre, and Coleman[11] measured the laser-intensity decay in the afterglow of a pulsed discharge in pure CO_2 for the $P(20)$ transition in the 9.4- and 10.4-μm bands. Over the pressure range 0.5–2.6 Torr of CO_2 the 9.4-μm decay was found to be characterized by a single exponential decay of $(0.8 \pm 0.25)\times 10^6$ sec^{-1} Torr^{-1}, and over the same pressure range, the 10.4-μm-pulse decay was governed by two exponentials having decay rates of $(1.05 \pm 0.3)\times 10^6$ sec^{-1} Torr^{-1} and $(1.4 \pm 0.5)\times 10^5$ sec^{-1} Torr^{-1}. They do not ascribe these rates to any specific molecular process but emphasize that they are phenomenological decay rates which "can only be related to the actual decay rates with more information or assumptions." Thus a comparison with the present work is not possible.

B. Comparison with theory

Two different theories describing vibrational energy transfer have been used to evaluate the collisional rate constant described by Eq. (1) in which M represents a ground-state CO_2 molecule. One of the calculations, performed by Seeber,[12] is based on the Schwarz, Slawsky, Herzfeld[13] (SSH) theory in which the strong, short-range repulsive forces are considered responsible for the energy exchange. The other approach developed by Sharma[9] is a Born-approximation formulation in which long-range forces determine the V-V

transfer. In Table I are listed the results from these descriptions for the relaxation of Eq. (1) and other pertinent CO_2-CO_2 collisional processes.

As is seen from Table I, Eq. (6), which corresponds to Eq. (1) with $M=CO_2(00^00)$, predicts rate constants for $k_{CO_2-CO_2}$ on either side of the measured value 3×10^5 sec^{-1} Torr^{-1}. Thus, a reformulation of these two theoretical approaches is warranted on the basis of this comparison. Recently, a less limiting approach by Dillon and Stephenson[14] uses a scattering-operator formalism to describe energy transfer between vibrationally excited HF, DF, HCl, and CO_2. They obtain excellent agreement with experiment. It is suggested that this alternate and more complete formulation of the V-V collisional exchange could be utilized to calculate a third $k_{CO_2-CO_2}$ value that stands in better agreement with the measured rate constant for Eq. (6). Such a calculation is not pursued in this paper. Furthermore, to our knowledge, no theoretical analysis has been attempted to predict rate constants for Eq. (1) in which M = He, or N_2.

We next discuss the signal shape in Fig. 3 lying between the fastest [process of Eq. (1)] and slowest components (00^01 collisional deactivation). As mentioned in Sec. III, the turnover in signal after the initial rise in Fig. 3 is attributed to re-equilibrations of the 02^00 level with other states that repopulate it. Such possible processes are identified in Eqs. (2) and (3). The rate constant for Eq. (2) was calculated by Seeber[12] and Sharma[9] and is listed in Table I [as Eq. (8)], with a value ~2.9 $\times10^4$ sec^{-1} Torr^{-1} at 400°K. Seeber determines a rate constant for Eq. (3) for $M=CO_2$ (not listed in Table I) to be ~8×10^4 sec^{-1} Torr^{-1} at 400°K. This latter value seems large since the process in Fig. 4 is well described by a single exponential function which must correspond to transfer of population out of the 02^00 state rather than transfer into it. However, the calculated rate constant for Eq. (2) is consistent with the signal in Fig. 3, being about an order of magnitude smaller than our measurements for the 02^00-10^00 relaxation. Recently Bulthuis and Ponsen,[15] using a method of measuring the relaxation time of the 10^00 level from the decay of the laser power in the afterglow of a CO_2-laser discharge, measured a rate constant for the reverse process of Eq. (9) in Table I and their findings are in accord with Seeber's predictions. This agreement adds confidence to the correctness of the calculated value for the process of Eq. (2).

For completeness, we note that one could reinterpret the relevant mechanism indicated by the signal trace in Fig. 4 and expressed by Eq. (1) to be instead due to the process

$$02^00 + 00^00 \rightarrow 02^20 + 00^00 - 49.9\ \text{cm}^{-1}, \qquad (11)$$

if the reaction

$$02^20 + 00^00 \rightarrow 10^00 + 00^00 - 52.7\ \text{cm}^{-1} \qquad (12)$$

proceeds at a rate significantly faster than that for Eq. (11). At least two arguments exist against this interpretation: (i) the rate constant for the reaction given by Eq. (12) is too slow relative to that of Eq. (11). As seen in Table I, Seeber calculates the rate constant for Eq. (12) to be 6.6×10^4 sec^{-1} Torr^{-1}(400°K), while Sharma determines the rate to be 1.7×10^5 sec^{-1} Torr^{-1}(400°K);

TABLE I. Calculated collisional rate constants for CO_2 considering short-range (Seeber) and long-range (Sharma) forces at 300 °K (400 °K in parentheses).

Process	Predicted rate constants (sec^{-1} Torr^{-1}) Seeber[a]	Sharma[b]
Eq. (6) $02^00 + 00^00 \rightarrow 10^00 + 00^00 - 102.8\ \text{cm}^{-1}$	4.5×10^4 (5.5×10^4)	$\geq 1\times10^6$[b]
Eq. (7) $02^20 + 00^00 \rightarrow 10^00 + 00^00 - 52.7\ \text{cm}^{-1}$	6.3×10^4 (6.6×10^4)	2.3×10^5 (~1.7×10^5)
Eq. (8) $01^10 + 01^10 \rightarrow 02^00 + 00^00 + 50.1\ \text{cm}^{-1}$	3.3×10^4 (3.2×10^4)	3.3×10^4 (~2.5×10^4)
Eq. (9) $01^10 + 01^10 \rightarrow 10^00 + 00^00 - 53.7\ \text{cm}^{-1}$	2.6×10^4 (2.7×10^4)	3.3×10^4 (~2.5×10^4)
Eq. (10) $01^10 + 01^10 \rightarrow 02^20 + 00^00 - 1.0\ \text{cm}^{-1}$	5.5×10^5 (6.0×10^5)	1.8×10^6 (~1.4×10^6)

[a] The rate constants at 400 °K are from K. N. Seeber (private communication). The values at 300 °K are from Ref. 12. Note that the factor for Eq. (8) in Ref. 12 should be 0.78 and not 0.6 as stated.

[b] R. D. Sharma (private communication). His rate-constant evaluations roughly decrease linearly with increasing temperature.

(ii) the measured rate constants for He and N_2 in Fig. 5 are comparable to the pure CO_2 value, thus removing the criticality of near-resonant interactions as expressed by Eq. (1) with $M=CO_2$ or Eqs. (11) and (12). Of course, this point could be answered experimentally if one probes the 02^20-level population by a second absorbed probe laser beam originating at this state, such as through the 02^20-04^20 transition at 8.05 μm or the 02^20-03^10 transition at 16.76 μm. We note that the process in Eq. (11) could also be interpreted to be the operative mechanism in the present experiment if Raman scattering from the 10^00 to 02^00 states is important. Stimulated Raman scattering is ruled out since the worst situation caused by this effect is an equalization of the 10^00 and 02^00 populations. In that case any re-equilibrating collisions would tend to increase the 02^00 density to its preperturbation value. In that situation, the signal shape of Fig. 4 would *decrease*—opposite to the observed behavior. On the other hand, resonantly enhanced spontaneous Raman scattering could produce the rising signal shape in Fig. 4 if Eq. (11) were the relevant collisional deactivation mechanism. Using a measured[16] (nonresonant) Raman cross section for CO_2 and suitably accounting for wavelengths, matrix elements, and the pressure-broadened linewidth of the 00^01 level, one can evaluate a generous upper limit due to resonant enhancement of the cross section. Even in this "worst possible" scenario, the percentage increase in the 02^00 density is less than 0.01%. Thus, Raman processes have no impact on the present rate-constant determinations.

ACKNOWLEDGMENTS

The authors thank Drs. W. H. Lowdermilk, K. R. Manes, and C. K. Rhodes for several helpful discussions.

---

*This work was performed under the auspices of the U.S. Atomic Energy Commission.

[1]There are three recent review articles dealing with various properties of the CO_2 molecule: (i) vibrational relaxation data in R. L. Taylor and S. Bitterman, Rev. Mod. Phys. 41, 26 (1969); (ii) summaries of CO_2 lasers and pulse propagation properties in P. K. Cheo, *Lasers 3*, edited by A. K. Levine and A. J. DeMaria (Dekker, New York, 1971), pp. 111–267; and (iii) O. R. Wood II, Proc. IEEE 62, 355 (1974).

[2]E. Fermi, Z. Phys. 71, 250 (1931). A description in English can be found in Ref. 1 (ii), for the 10^00 and 02^00 mixing.

[3]R. R. Jacobs, S. J. Thomas, and K. J. Pettipiece, IEEE J. Quantum Electron. QE-10, 480 (1974).

[4]R. R. Jacobs, Rev. Sci. Instrum. 44, 1146 (1973).

[5]E. F. Worden (private communication). The relative intensity of the 9.4-μm to 10.4-μm component from the actively mode-locked laser could be changed by addition of various amounts of SF_6 gas into the oscillator cavity.

[6](i) An induced-fluorescence technique to determine the 00^01 relaxation rate constant was used in: (a) L. O. Hocker, M. A. Kovacs, C. K. Rhodes, G. W. Flynn, and A. Javan, Phys. Rev. Lett. 17, 233 (1966) (k_{0001} = 385 sec^{-1} $Torr^{-1}$); (b) C. B. Moore, R. E. Wood, B. Hu, and T. J. Yardley, J. Chem. Phys. 46, 4222 (1967) (k_{0001} = 350 sec^{-1} $Torr^{-1}$). (ii) An afterglow pulse gain technique was utilized in P. K. Cheo, J. Appl. Phys. 38, 3563 (1967) (k_{0001} = 385 sec^{-1} $Torr^{-1}$).

[7]R. R. Jacobs, K. J. Pettipiece, and S. J. Thomas, Appl. Phys. Lett. 24, 375 (1974).

[8]E. E. Stark, Jr., Appl. Phys. Lett. 23, 335 (1973).

[9]R. D. Sharma, J. Chem. Phys. 49, 5195 (1968).

[10]C. K. Rhodes, M. J. Kelley, and A. Javan, J. Chem. Phys. 48, 5730 (1968).

[11]T. A. DeTemple, D. R. Suhre, and P. D. Coleman, Appl. Phys. Lett. 22, 349 (1973).

[12]K. N. Seeber, J. Chem. Phys. 55, 5077 (1971).

[13]R. N. Schwartz, Z. I. Slawsky, and K. F. Herzfeld, J. Chem. Phys. 20, 1591 (1952).

[14]T. A. Dillon and J. C. Stephenson, J. Chem. Phys. 58, 2056 (1973).

[15]K. Bulthuis and G. J. Ponsen, Chem. Phys. Lett. 14, 613 (1972).

[16]D. G. Fouche and R. K. Chang, Appl. Phys. Lett. 18, 579 (1971).

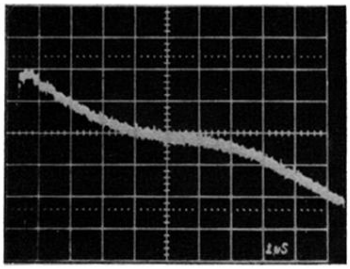

FIG. 3. Shown is an oscilloscope trace for the transmitted $P(24)$ 9.4-μm probe-beam intensity subsequent to absorption of the 10.4-μm pulse for a CO_2 pressure of 100 Torr. The rapid initial rise corresponds to the mechanism given by Eq. (1). The other signal features are discussed in the text.

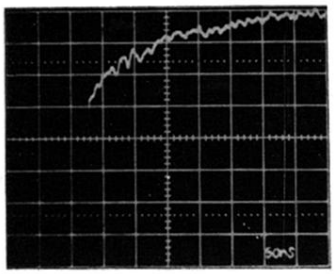

FIG. 4. Depicted is a typical oscilloscope trace for the $02^00\text{-}10^00$ relaxation in CO_2 (50 Torr). This signal is an expansion of the initial signal rise in Fig. 3. Note that the probe laser baseline is offset from view in Figs. 3 and 4.